Supplementary Materials

Decorating pore environment via cationic units of covalent organic frameworks for enhancing CO_2 reduction reaction

Minghao Liu[1,2], Guojuan Liu[1,3], Qing Xu[1,3,*], Gaofeng Zeng[1,3,*]

[1]CAS Key Laboratory of Low-Carbon Conversion Science and Engineering, Shanghai Advanced Research Institute (SARI), Chinese Academy of Sciences (CAS), Shanghai 201210, China.
[2]Department of Chemical and Environmental Engineering, University of Nottingham Ningbo China, Ningbo 315199, Zhejiang, China.
[3]University of Chinese Academy of Sciences, Beijing 100049, China.

[*]**Correspondence to:** Prof. Qing Xu, CAS Key Laboratory of Low-Carbon Conversion Science and Engineering, Shanghai Advanced Research Institute (SARI), Chinese Academy of Sciences (CAS), 99 Haike Road, Shanghai 201210, China. E-mail: xuqing@sari.ac.cn; zenggf@sari.ac.cn

Experimental Procedures

Characterizations

Powder X-ray diffraction (PXRD) data were recorded on a Rigaku model RINT Ultima III diffractometer by depositing powder on glass substrate, from 2θ = 3° up to 30° with 1° increment. Nitrogen sorption isotherms were measured at 77 K with a Micromeritics Instrument Corporation model 3Flex surface characterization analyzer. The Brunauer-Emmett-Teller (BET) method was utilized to calculate the specific surface areas. By using the non-local density functional theory (NLDFT) model, the pore volume was derived from the sorption curve. FE-SEM images were obtained on a FEI Sirion-200 or Hitachi high technologies (SU-6600) field-emission scanning electron microscope at an electric voltage of 5 KV. EDX and elemental mapping were acquired using a HITCHI Miniscope TM3030. High-resolution transmission electron microscope images were obtained by transmission electron microscopy (TEM, FEI Tecnai G2). ICP was performed on a Perkin-Elmer Elan DRC II Quadrupole Inductively Coupled

Plasma Mass Spectrometer (ICP-MS) analyzer. Fourier transform infrared (FT-IR) spectroscopy was measured using KBr pellets on a Perkin Elmer Spectrum 100 spectrometer in the 500-4,000 cm^{-1}. UV-vis absorbance spectra were recorded on a Cary 5000 UV-vis-NIR spectrophotometer equipped with a mercury lamp. Substrates were mixed with $BaSO_4$. Base line correction was done towards $BaSO_4$. Spectra were taken over a wavelength range of 200-1200 nm with a 5 min collection time and 1 nm resolution. The Tauc plots were calculated based on the UV-Vis spectra data. The cobalt content of samples was obtained using inductively coupled plasma optical emission spectroscopy (ICP-OES) on an Optima 8000 spectrometer.

Pawley refinement

The powder X-ray diffraction (PXRD) pattern simulation was performed using a software package for crystal determination from PXRD pattern, implemented in Reflex module of Materials Studio. We performed Pawley refinement to optimize the lattice parameters iteratively until the R_P and R_{WP} values converge. The pseudo-Voigt profile function was used for whole profile fitting and Finger-Cox-Jephcoat function was used for asymmetry correction during the refinement processes.

Materials

All the chemicals commercially available were used without further purification. 4,4',4",4"'-(1,4-phenylenebis(azanetriyl))tetrabenzaldehyde, 5,10,15,20-tetrakis(4-aminophenyl)porphinato]-cobalt and (3-carboxypropyl)trimethylammonium and were obtained from Alfa. Acetic acid, *o*-Dichlorobenzene (*o*-DCB, > 99%), tetrahydrofuran (THF, > 97%), acetone (> 97%) and n-Butanol (BuOH, > 97%) were obtained from Sinopharm Chemical Reagent Co.,Ltd.

Synthesis of Co-COF

A mixture of *o*-DCB and BuOH (0.5/0.5/0.1 mL), 4,4',4",4"'-(1,4-phenylenebis(azanetriyl))tetrabenzaldehyde (0.02 mmol), 5,10,15,20-tetrakis(4-aminophenyl)porphinato]-cobalt (0.02 mmol), and an aqueous acetic acid solution (6 M, 0.1 mL) was degassed in a Pyrex tube (10 mL) by three

freeze-pump-thaw cycles. The tube was sealed and heated at 120 °C for 3 days. The precipitate was collected by centrifugation, washed with THF, and dried at 120 °C under vacuum for 6 h to give Co-COF in a yield of 80.5%.

Synthesis of TMA-COF

A mixture of *o*-DCB, BuOH and EtOH (0.5/0.5/0.1 mL), 4,4',4'',4'''-(1,4-phenylenebis(azanetriyl))tetrabenzaldehyde (0.015 mmol), 5,10,15,20-tetrakis(4-aminophenyl)porphinato]-cobalt (0.03 mmol), (3-carboxypropyl)trimethylammonium (0.015 mmol) and an aqueous acetic acid solution (6 M, 0.1 mL) was degassed in a Pyrex tube (10 mL) by three freeze-pump-thaw cycles. The tube was sealed and heated at 120 °C for 3 days. The precipitate was collected by centrifugation, washed with THF and acetone, and dried at 120 °C under vacuum for 6 hours to give TMA-COF in a yield of 79.4%.

Electrochemical performance tests

The preparation of working electrode 5 mg COFs and 5 mg carbon nanotube was grinded for 60 min and dispersed in mixed solution of 50 μL Nafion solution (5 wt%), ethanol (950 μL) followed with sonication for 120 min. The 200 μL as-prepared catalyst ink was directly spray-coated on a hydrophobic carbon paper (1 cm × 1 cm) to form a 1 cm^2 catalyst area with a catalyst loading of 1 $mg \cdot cm^{-2}$. In addition, the carbon paper with the thickness was 0.37 mm. The deposited carbon paper was further dried at room temperature. All the electrochemical experiments were performed in a H-type cell with two-compartments separated by an anion exchange membrane (Nafion-117). Each compartment contained 50 mL electrolyte (0.5 M $KHCO_3$). Electrochemical measurements were performed in a three-electrode cell using the Ag/AgCl electrode as the reference electrode and Pt foil as the counter electrode on the electrochemical instrument (CHI760E). Before the electrochemical measurements, the electrolyte solution was purged with CO_2 for 30 min to obtain the CO_2-saturated solution. A mass flow controller was used to set the Ar or CO_2 flow rate at 20. The LSV curves were conducted with scan rate of 10 mV/s. All the potentials were reported with respect to the reversible hydrogen electrode (RHE) and conversed using the formula E (*vs*. RHE) = E (*vs*. Ag/AgCl) + 0.196 V +0.059 × pH.

The calculation of Faradic efficiency.

$$FE = \frac{N \times F \times n_{CO}}{I \times 60\ (s/min)} \times 100\%$$

Where F is the Faraday constant; n_{CO} is the moles of produced CO; I is total steady-state cell current; N is the electron transfer number for product formation.

Turnover frequency (TOF)

The turnover frequency (TOF) was evaluated by the following standard equation:

$$TOF = (J \times A)/(2 \times F \times n)$$

Where *j* (A/cm^2) is the partial current for certain product; A is the geometric surface area of the electrode; *F* stands for the Faraday constant; *n* (mol) is molar amount of cobalt loaded on the GC electrode which was determined by the ICP analysis.

All metal cations in the COFs were assumed to be catalytically active, so the calculated value represents the lower limits of the TOF.

Mott-Schottky curve test

Preparation of working electrode: 2 mg COF powder was mixed with 0.45 mL ethanol and 0.05 mL Nafion (5%) dispersion, and ultrasonic treatment was performed for 60 min. The resulting mixture slurry is evenly coated on the bottom of the ITO glass plate in the 1 × 2 cm^2 area, and placed in the air to stand for drying naturally.

Electrochemical test for Mott-Schottky curve

Electrochemical measurements were performed in a three-electrode cell using the Ag/AgCl electrode as the reference electrode. Using 500 and 1,000 Hz to test the curve.

Results and Discussion

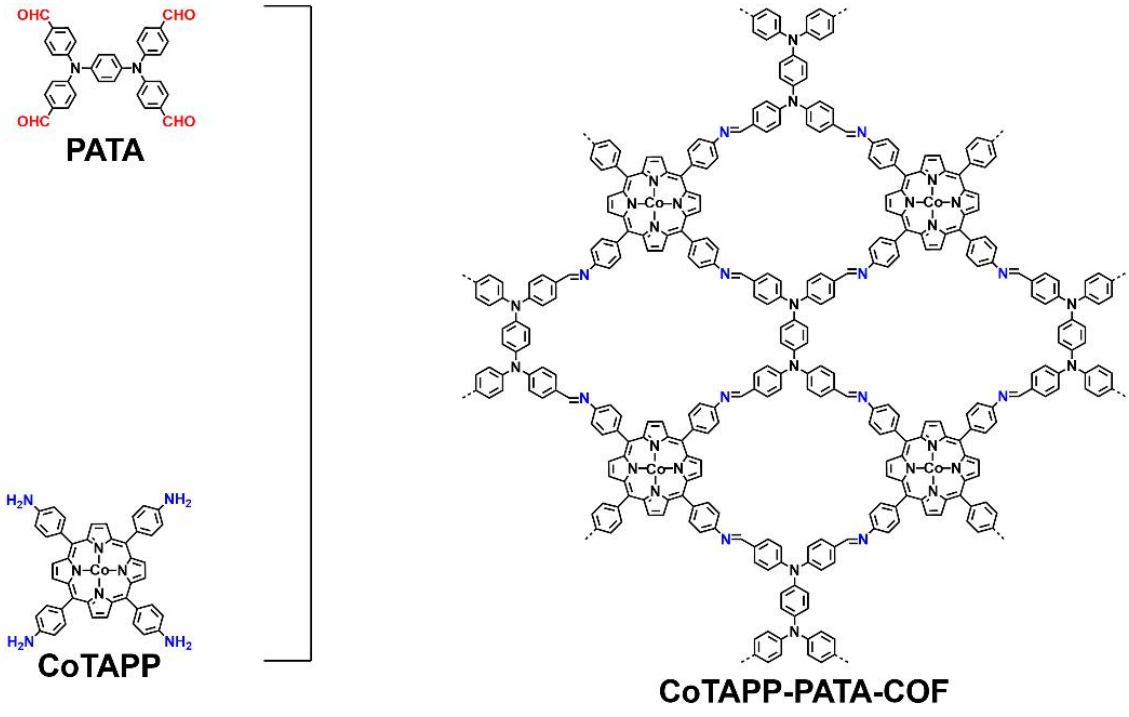

Supplementary Figure 1. The scheme of synthesis for Co-COF.

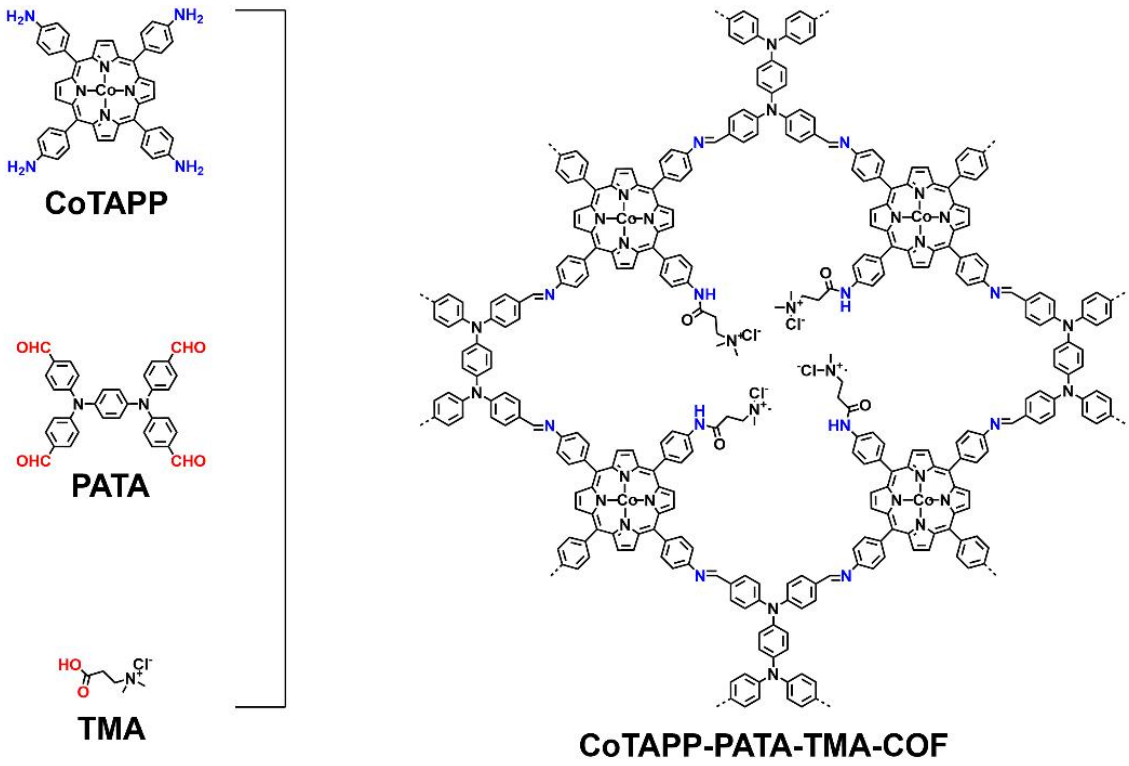

Supplementary Figure 2. The scheme of synthesis for TMA-COF.

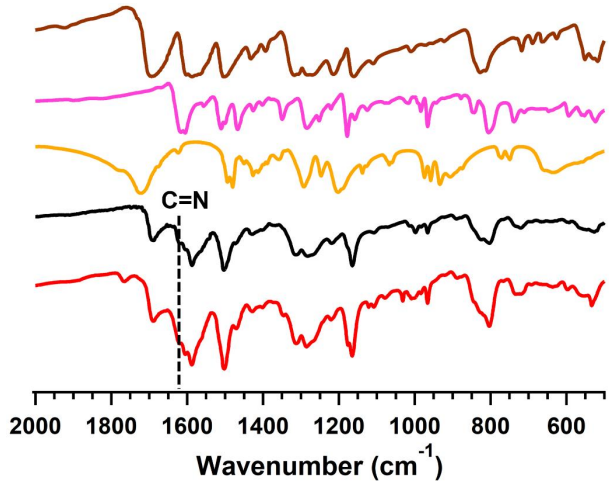

Supplementary Figure 3. FT IR spectra of PATA (brown), CoTAPP (pink), TMA (orange), Co-COF (black) and TMA-COF (red).

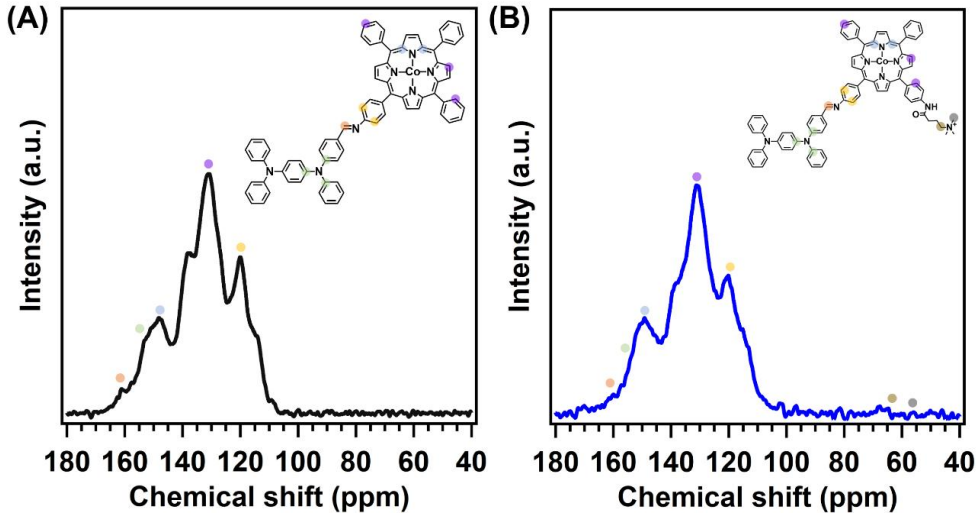

Supplementary Figure 4. The ^{13}C NMR spectra of (A) Co-COF and (B) TMA-COF.

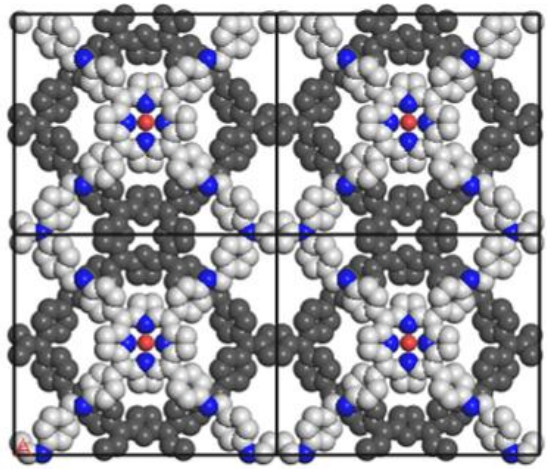

Supplementary Figure 5. Staggered-AB model of Co-COF for top view.

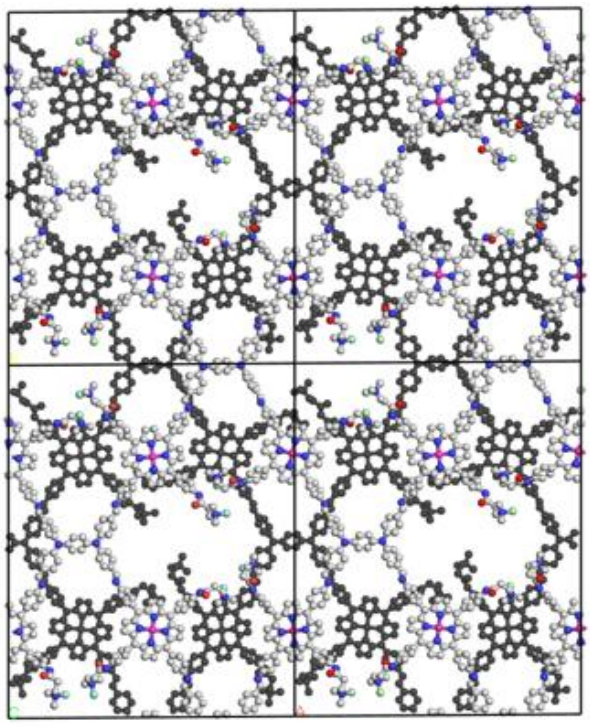

Supplementary Figure 6. Staggered-AB model of TMA-COF for top view.

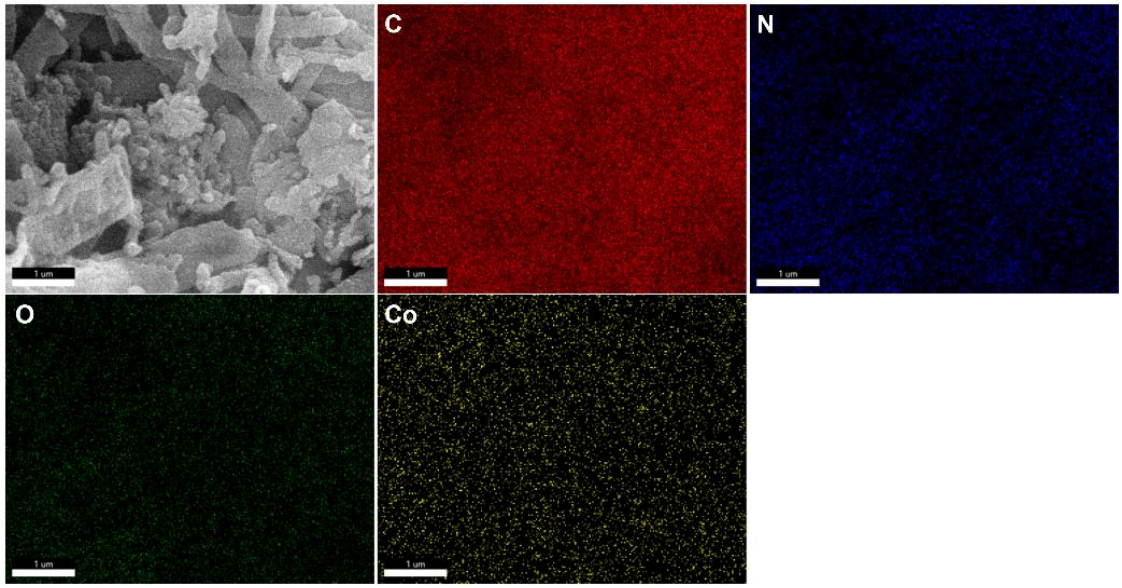

Supplementary Figure 7. EDX mapping images of Co-COF.

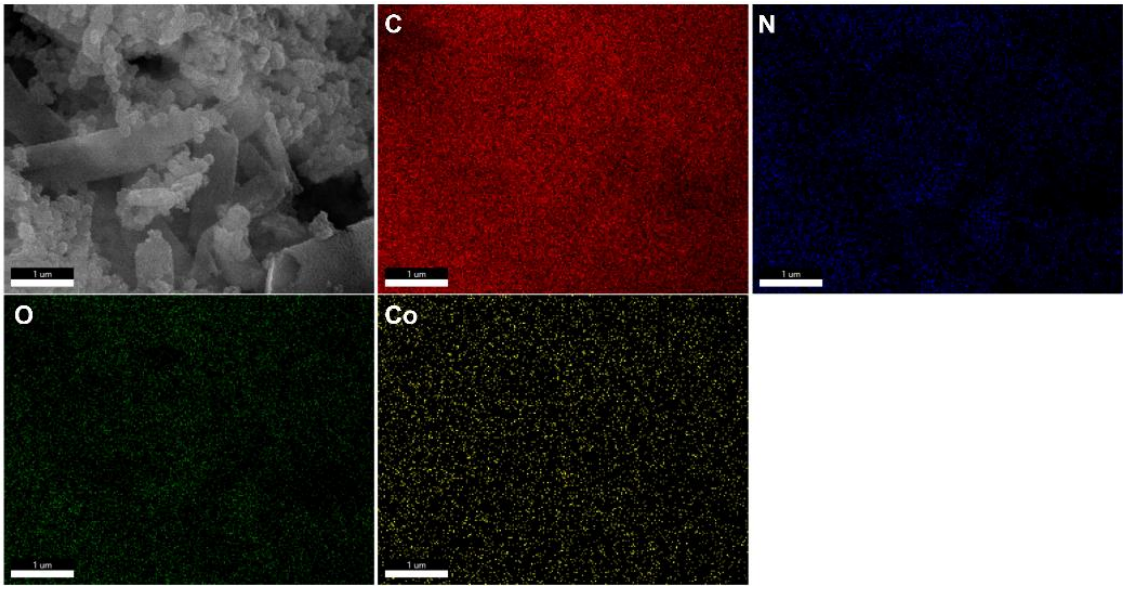

Supplementary Figure 8. EDX mapping images of TMA-COF.

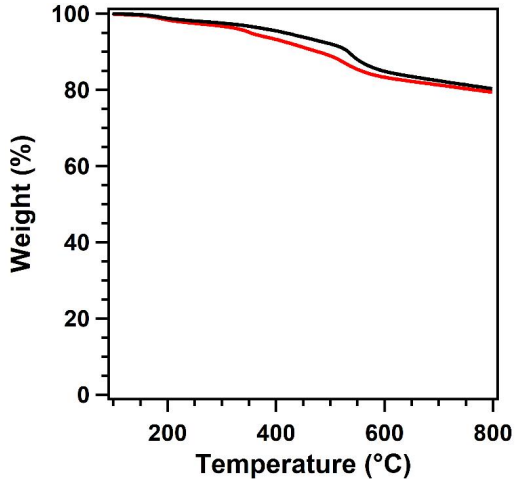

Supplementary Figure 9. TGA curves of Co-COF (black) and TMA-COF (red) under nitrogen atmosphere.

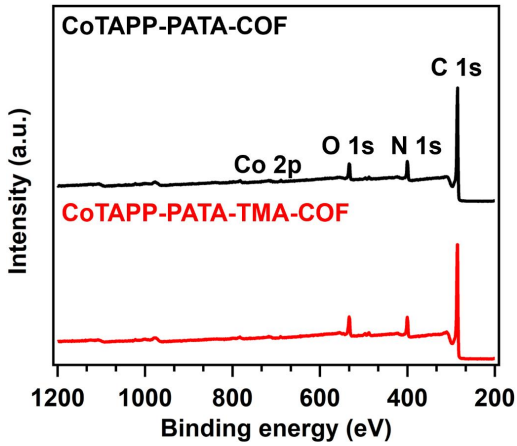

Supplementary Figure 10. The XPS spectra of Co-COF (black) and TMA-COF (red).

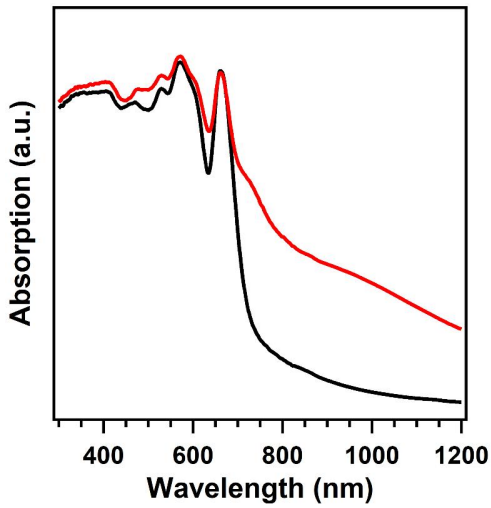

Supplementary Figure 11. The UV-Vis spectra of Co-COF (black) and TMA-COF (red).

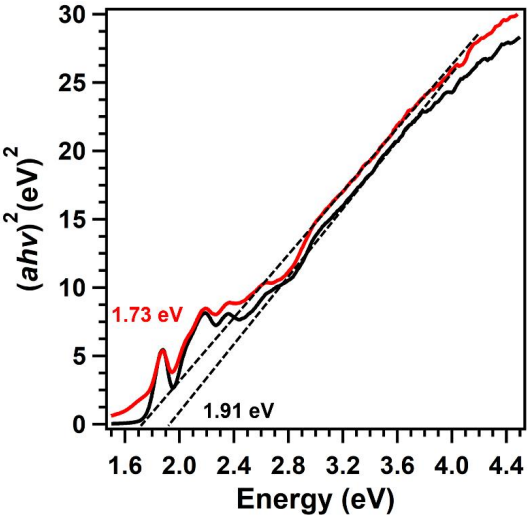

Supplementary Figure 12. The Tauc plots of Co-COF (black) and TMA-COF (red).

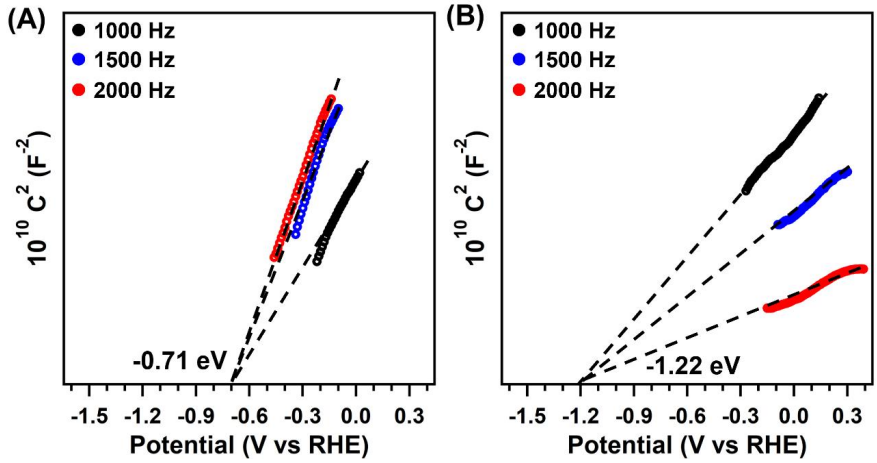

Supplementary Figure 13. Mott–Schottky plots of (A) Co-COF and (B) TMA-COF from 1000 Hz to 2000 Hz.

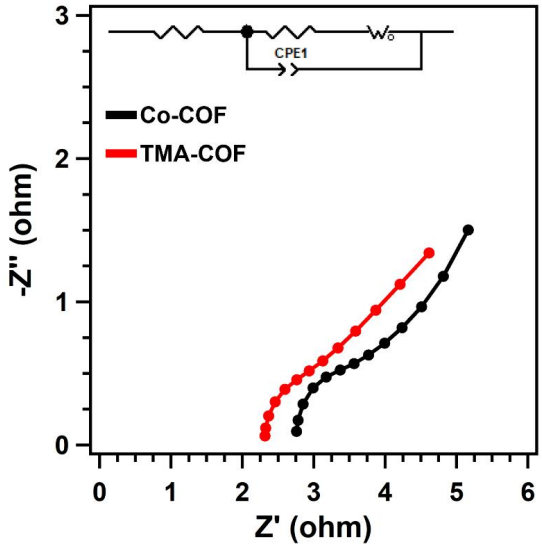

Supplementary Figure 14. The Nyquist plots of Co-COF (black) and TMA-COF (red) on the carbon paper with carbon nanotubes in 0.5 M $KHCO_3$.

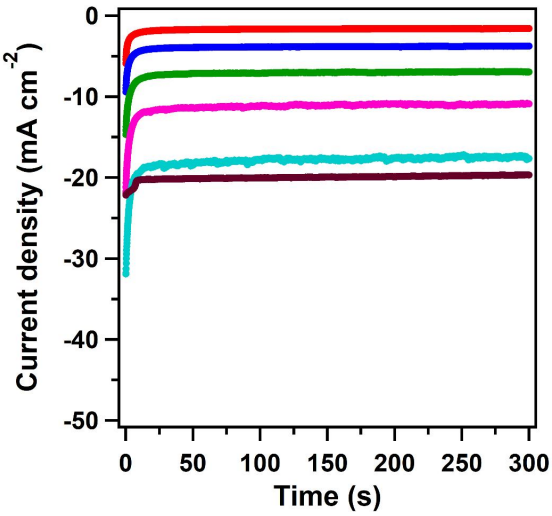

Supplementary Figure 15. Chronoamperometric responses of Co-COF, at –0.5 (red), –0.6 (blue), –0.7 (green), –0.8 (pink), –0.9 (cyan), and –1.0 V (brown) (vs. RHE).

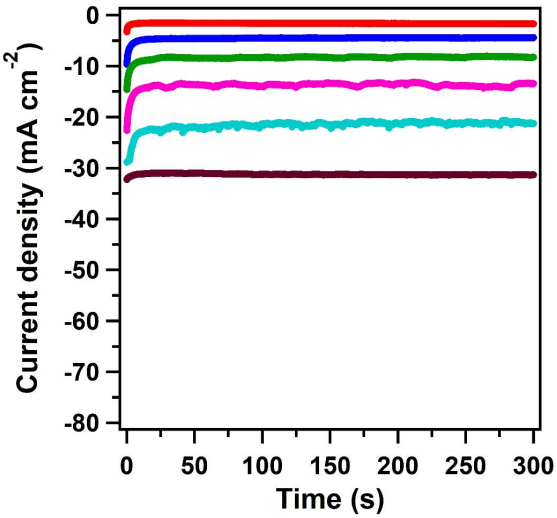

Supplementary Figure 16. Chronoamperometric responses of TMA-COF, at -0.5 (red), -0.6 (blue), -0.7 (green), -0.8 (pink), -0.9 (cyan), and -1.0 V (brown) (*vs*. RHE).

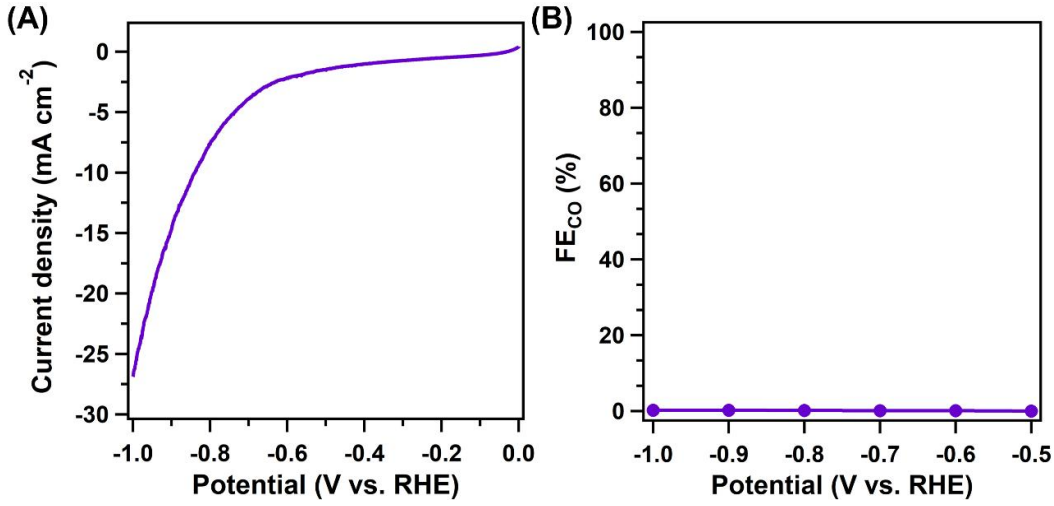

Supplementary Figure 17. (A) The LSV curves and (B) FE_{CO} curves of CNTs from -0.5 to -1.0 V in 0.5 M $KHCO_3$ under CO_2 atmosphere.

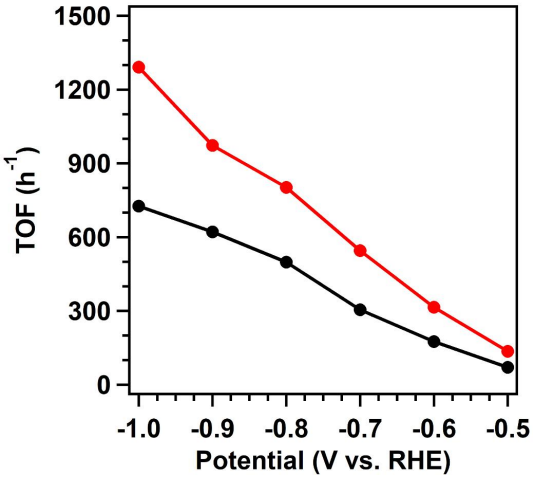

Supplementary Figure 18. The TOF values of Co-COF (black) and TMA-COF (red).

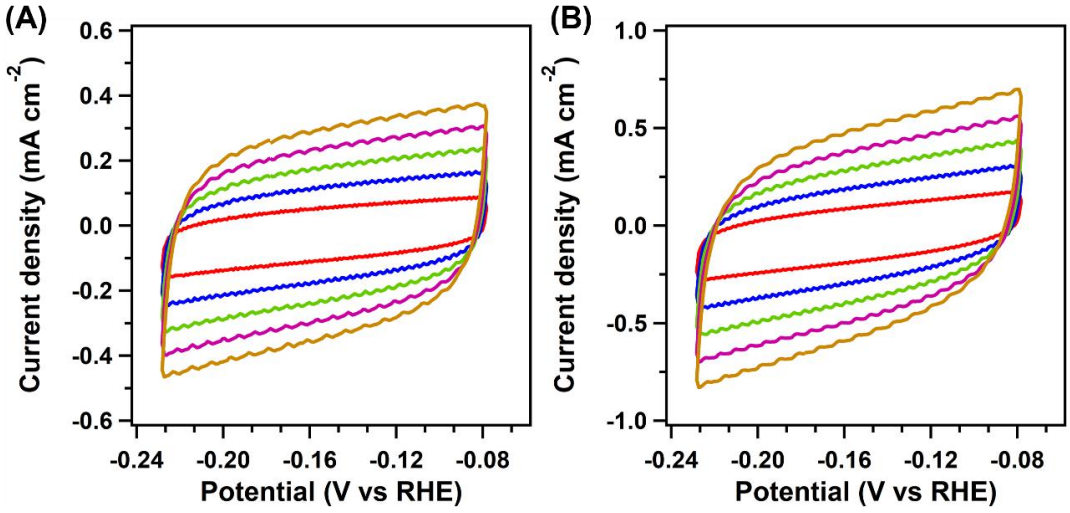

Supplementary Figure 19. The CV curves from 10 mV s^{-1} to 50 mV s^{-1} for (A) Co-COF and (B) TMA-COF.

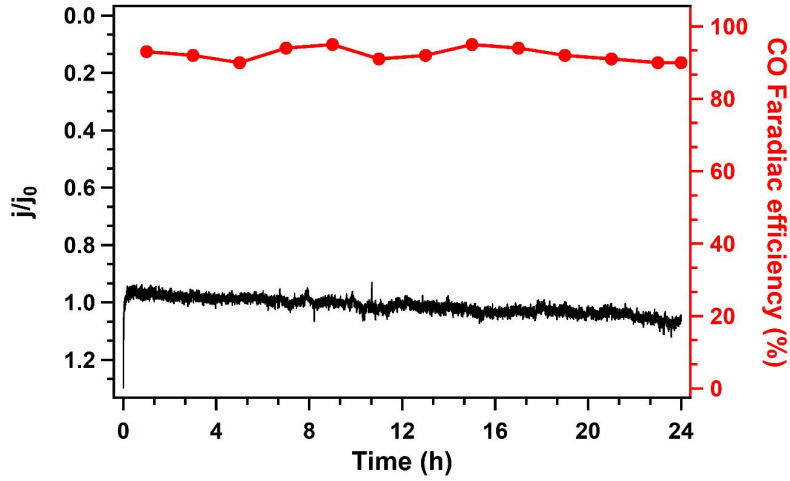

Supplementary Figure 20. The long-term stability tests of TMA-COF with the change of FE_{CO} (red) and current density (black).

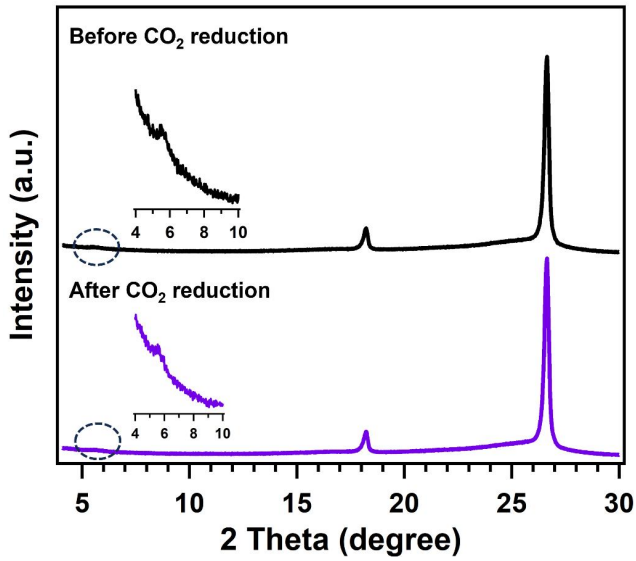

Supplementary Figure 21. The PXRD patterns of COFs with CNT coating on the carbon paper before (black) or after (purple) the long-term stability tests.

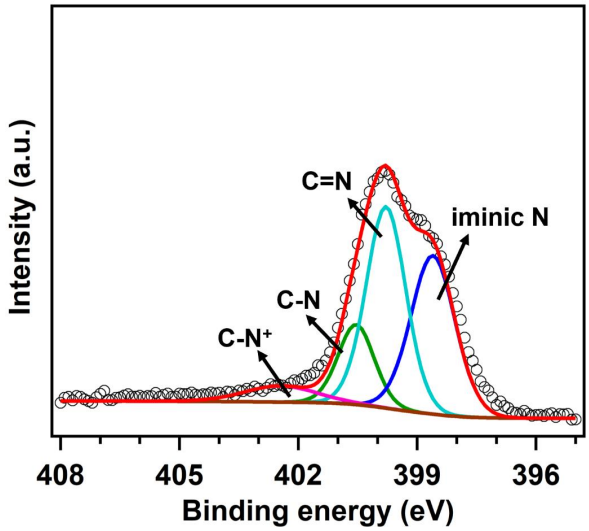

Supplementary Figure 22. The XPS spectra of N 1s for TMA-COF after the long-term stability tests.

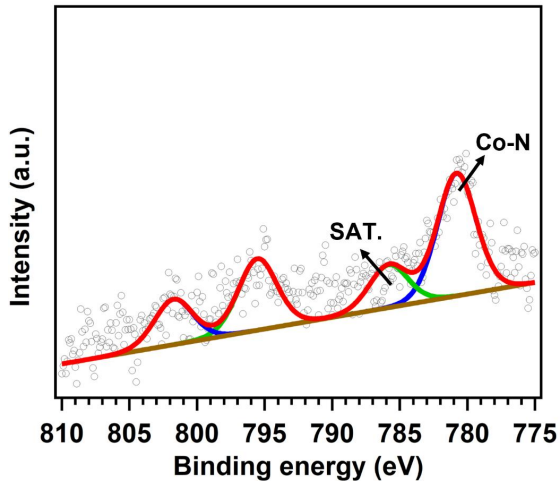

Supplementary Figure 23. The XPS spectra of Co 2p for TMA-COF after the long-term stability tests.

Supplementary Table 1. Summary of recently reported CO_2RR performances of other reported COF derived electrocatalysts under alkaline conditions (Electrolyte 0.5 M $KHCO_3$).

Electrocatalyst	**FE_{CO} (%) at -0.8 V**	**j_{CO} ($mA \cdot cm^{-2}$) at -1.0 V**	**Ref.**
Co-COF	82	12.9	**This work**
TMA-COF	95	24.6	**This work**
COF-367-Co	91	33.0	[1]
CoPc-PI-COF-1	95	21.2	[2]
CoPc-PI-COF-2	92	~15	[2]
CoP-BDT_{HexO}-COF	98	10.8	[3]
TAPP(Co)-B18C6-COF	93	9.5	[4]
COF@CoPor	88.5	12.5	[5]
COF-300-AR	80	-	[6]
Co-TTCOF	~88	~2.5	[7]
TT-Por(Co)-COF	~87	~5.6	[8]
CoPc-BP-COF	89	24.1	[9]
NiPc-COF	93	35.0	[10]

References

[1]. Lin, S. et al. Covalent organic frameworks comprising cobalt porphyrins for catalytic CO_2 reduction in water. *Science* **349**, 1208-1213 (2015). [DOI: 10.1126/science.aac8343]

[2]. Han, B. et al. Two-Dimensional Covalent Organic Frameworks with Cobalt(II)-Phthalocyanine Sites for Efficient Electrocatalytic Carbon Dioxide Reduction. *J. Am. Chem. Soc.* **143**, 7104-7113 (2021). [DOI: 10.1021/jacs.1c02145]

[3]. He, T. et al. Bottom-Up Interfacial Design of Covalent Organic Frameworks for Highly Efficient and Selective Electrocatalysis of CO_2. *Adv. Mater.* **34**, 2205186 (2022). [DOI: 10.1002/adma.202205186]

[4]. An, S. et al. Constructing Catalytic Crown Ether-Based Covalent Organic Frameworks for Electroreduction of CO_2. *ACS Energy Lett.* **6**, 3496-3502 (2021). [DOI: 10.1021/acsenergylett.1c01681]

[5]. Zhai, L. et al. CoN_5 Sites Constructed by Anchoring Co Porphyrins on Vinylene-Linked Covalent Organic Frameworks for Electroreduction of Carbon Dioxide. *Small* **18**, 2200736 (2022). [DOI: 10.1002/smll.202200736]

[6]. Liu, H. et al. Covalent Organic Frameworks Linked by Amine Bonding for Concerted Electrochemical Reduction of CO_2. *Chem* **4**, 1696-1709 (2018). [DOI: 10.1016/j.chempr.2018.05.003]

[7]. Zhu, H.-J. et al. Efficient electron transmission in covalent organic framework nanosheets for highly active electrocatalytic carbon dioxide reduction. *Nat. Commun.* **11**, 497 (2020). [DOI: 10.1038/s41467-019-14237-4]

[8]. Wu, Q. et al. Construction of Donor–Acceptor Heterojunctions in Covalent Organic Framework for Enhanced CO_2 Electroreduction. *Small* **17**, 2004933 (2021). [DOI: 10.1002/smll.202004933]

[9]. Liu, M. et al. Ladder type covalent organic frameworks constructed with natural units for the oxygen and carbon dioxide reduction reactions. *Chem. Eng. J.* **488**, 150812 (2024). [DOI: 10.1016/j.cej.2024.150812]

[10]. Zhang, M.-D. et al. Conductive Phthalocyanine-Based Covalent Organic Framework for Highly Efficient Electroreduction of Carbon Dioxide. *Small* **16**, 2005254 (2020). [DOI: 10.1002/smll.202005254]